International Journal of Advances in Electrical Engineering

E-ISSN: 2708-4582
P-ISSN: 2708-4574
IJAEE 2024; 5(2): 42-51

www.electricaltechjournal.com
Received: 13-06-2024
Accepted: 20-07-2024

Chandragupta Mauryan KS
Guru Nanak Institution Technical Campus, Hyderabad, Telangana, India

Maloth Naresh
Guru Nanak Institute of Technology, Hyderabad, Telangana, India

R Purrnimaa Shiva Sakthi
Guru Nanak University, Hyderabad, Telangana, India

Correspondence
Chandragupta Mauryan KS
Guru Nanak Institution Technical Campus, Hyderabad, Telangana, India

Smart controller design for frequency control of an integrated microgrid

Chandragupta Mauryan KS, Maloth Naresh and R Purrnimaa Shiva Sakthi

DOI: https://doi.org/10.22271/27084574.2024.v5.i2a.72

Abstract
Frequency variations are caused by load deviations and renewable energy sources in a microgrid. These variations could result in system instability and large fluctuations of frequency and voltage in a microgrid. The microgrid considered here consists of conventional generator, renewable energy sources and battery energy storage system. This paper deals with designing robust controller to cope up with frequency variations in the microgrid. We develop PID, µ-synthesis, FOPID and SMC controller where robustness to uncertainties and disturbances are compared for system frequency fluctuations. All the simulations are conducted in the MATLAB™ and simulink™.

Keywords: Battery storage system, fractional order PID, load frequency deviations, microgrid, sliding mode control, µ-synthesis

Introduction
Microgrids are electricity distribution systems containing loads and distributed energy resources (such as distributed generators, storage devices or controllable loads) that can be operated in a controlled, coordinated way either while connected to the main power network or while islanded [1]. Microgrid offers distinct advantages to customers and utilities like improved energy efficiency, minimization of overall energy consumption, reduced environmental impact, improvement of reliability of supply, network operational benefits such as loss reduction, congestion relief, potentially reducing carbon footprint, make RTO markets more competitive, voltage control or security of supply and more cost efficient electricity infrastructure replacement. In-order to improve the efficiency of microgrid and reduce the fossil fuel consumption, renewable energy sources like wind, solar, tidal, biomass, hydro, etc. are combined with traditional microgrids. However, among all the renewable energy sources, wind turbine generator (WTG) system is one of the fastest growing, cost effective and clean power system [2]. Due to erratic behaviour of wind velocity, it affects system stability and causes fluctuations in frequency and voltages as the power output obtained from wind turbine generator is proportional to cube of the wind speed.
This paper mainly deals with reducing the deviations of frequency caused by WTG. One way of reducing frequency deviations is by installing battery storage systems. Battery sizes plays prominent role as there arises a problem regarding saturation at transients and of high cost. Under such situations, traditional methods for controlling the deviations become complex as battery size should be considered. Many algorithms for controlling fluctuations have been proposed to achieve better performance in spite of abrupt disturbances and model uncertainties. PID controller have been proposed but it has limited ability to tradeoff overshoot, rise time and damping oscillations [3]. Another controlling method deals with H infinity (H_∞) analysis overcoming limitations of PID controller but fails in responding robustness to uncertainties [4]. Fuzzy logic control is also been used but there arises difficulty in developing a simulation model which requires fine tuning of the controller [5].
Our motive is to develop robust control strategies for both battery and conventional generation systems, with controllers developed to reduce the battery size also reducing frequency deviations inspite of variable loads and including wind turbine generator (WTG) in the microgrid. They are compared with conventional PID controller and comes to the conclusion that a storage system with less size can extremely reduce the frequency

variations. This can be possible by avoiding saturation conditions where storage systems are coordinated with other generating sources, using Multi Input Multi Output (MIMO) control techniques. This paper introduces μ-synthesis approach as it has answered robustness to uncertainities in the system [6]. But it involves proper selection of performance weights. Modified performance weights could result in saturation of battery storage making system sluggish in nature. FOPID and SMC controller is used where better performance is obtained order to avoid such complexity for reducing frequency deviations in microgrid regardless system uncertainties [7, 8].

This paper mainly focus on comparison between controllers such as PID, μ-synthesis, FOPID and SMC on reducing frequency deviations in micro-grid. Rest of the paper is modelled as system strategy in section II, control design in section III, simulation results in section IV and conclusion in section V. The system considered in this paper consists of a microgrid [16, 17] which includes conventional generator, renewable energy sources, variable loads and attached storage system which is shown in Fig.1.

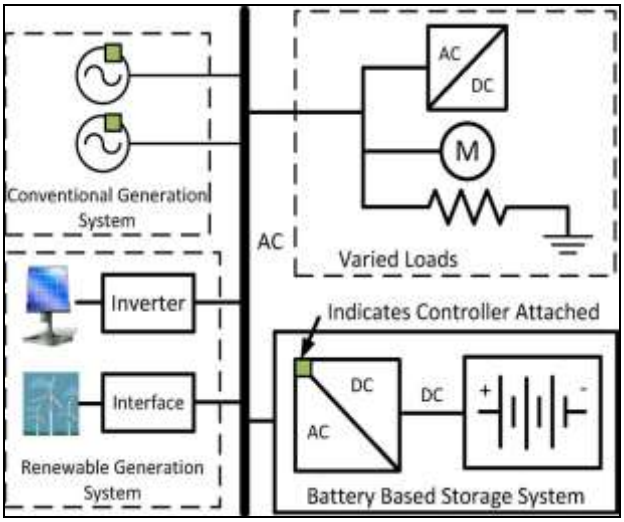

Fig 1: Structure of microgrid with attached storage system

The green block represents that respective component is under control for obtaining better performance. As microgrid incorporates various sources which could affect system stability due to frequency variations [18]. These frequency deviations are mainly due to wind generator and variable load. Low frequency deviations are handled by conventional generators and high frequency deviations are handled by battery storage system as they respond more quickly to load transients. In order to maintain rated frequency, advanced controllers are required to obtain good system performance [19, 20].

System strategy

A mathematical model is proposed here which comprises of three parts namely conventional generator, battery storage system and wind turbine generator where the corresponding simulink models are shown in figs. 2-4. The transfer functions used here are simple for reducing system complexity. All the signals in this model are considered in per unit (pu) basis and considering rated frequency as 60Hz. The load changes, battery output variations and WTG output variations are represented as: ΔP_{load}, ΔP_{batt} and ΔP_{wind} respectively. These three signals are summed at the summing block in the conventional generator model along with the output power variations denoted by ΔP_{gen} [9]. Note that during charging or discharging periods, battery energy storage system acts as load or generation accordingly

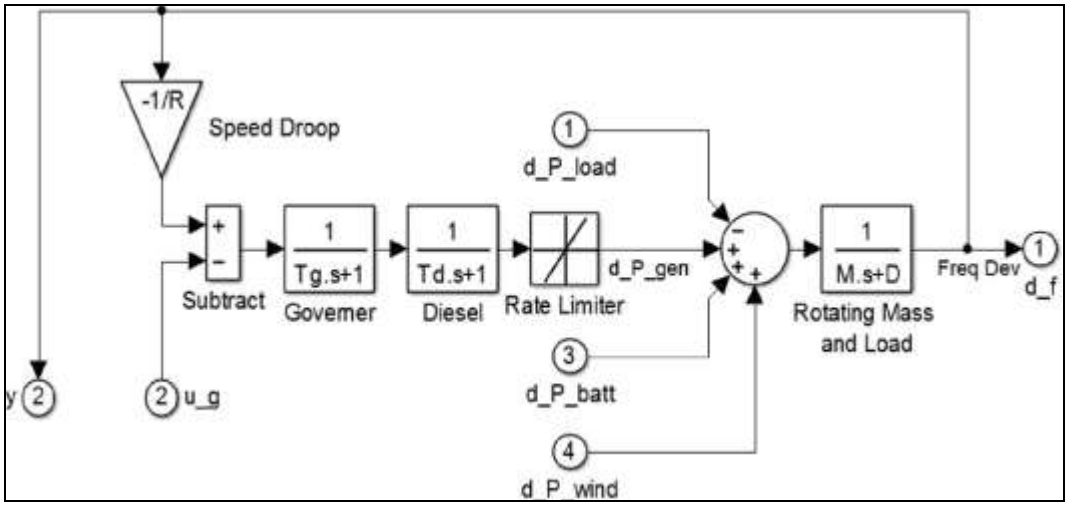

Fig 2: Conventional generator model

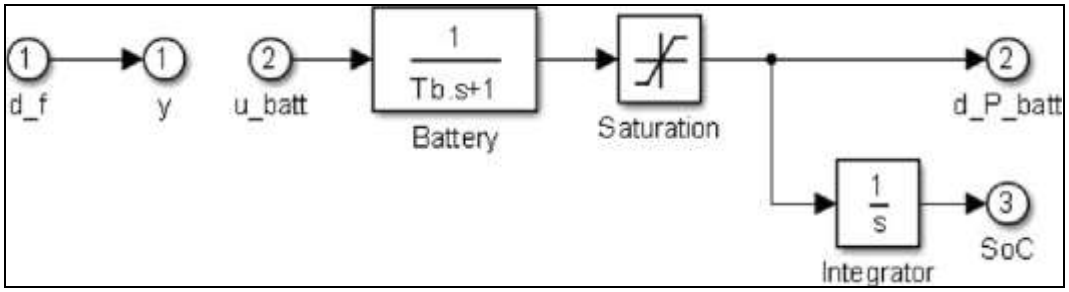

Fig 3: Battery model

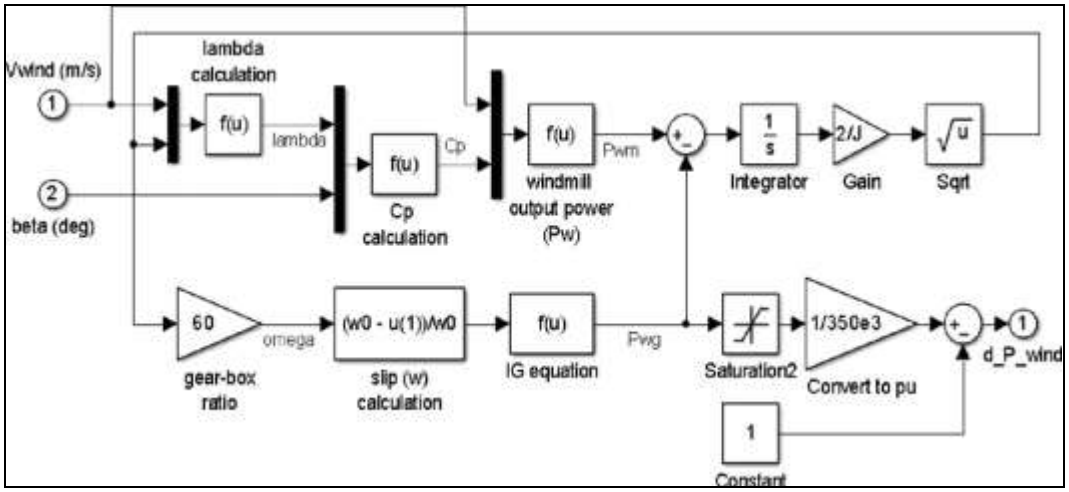

Fig 4: Wind turbine generator model

Here, ΔP_{batt} and ΔP_{gen} are controlled power deviations, 'u_g' and 'u_{batt}' are control signals, Δf is considered as the error signal. The controller receives measurements 'y' and output control signals 'u'. Saturation block is attached to battery model to prevent battery from fast charge and discharge. Additionally, state of charge (SOC) variation of the battery model is obtained by output power deviation which is controlled indirectly by commanding ΔP_{batt}. ΔP_{load} and ΔP_{wind} are considered as perturbations to the system in μ-synthesis and there is no control over these two signals. Here, the controlled outputs are used for minimizing Δf, in spite of varying perturbations. Other renewable sources can also be handled in similar way.

The block diagram of wind turbine generator is shown in fig. 4. Windmill output (P_{wm}) is determined by wind speed and pitch angle (β) [2]. The equation for P_{wm} is given by,

$$P_{wm} = C_p(\lambda,\beta) V_w^3 \rho A/2 \quad (1)$$

Tip speed ratio (λ) and coefficient of power (C_p) is given by,

$$\lambda = \frac{R_w \omega}{V_w} \quad (2)$$

$$C_p = \frac{1}{2}\left(\lambda - 0.022\beta^2 - 5.6\right)e^{-0.17\lambda} \quad (3)$$

The expression for WTG output (P_{wg}) is given as follows,

$$P_{wg} = \frac{-3V^2 S(1+S)R_2}{\left(R_2 - S R_2\right)^2 + S^2\left(X_1 + X_2\right)^2} \quad (4)$$

Where 'S' is the slip and is given by,

$$S = \frac{\omega_o - \omega}{\omega_o} \quad (5)$$

Where V_w is the wind speed, A is windmill rotor cross-section area, ω_0 is synchronous angular speed and ω is angular rotor speed of windmill. The controller doesn't have any control action on WTG as it is considered as disturbance. Hence we specify wind speed (V_w) as 12m/s and pitch angle (β) as 10^0. The modelling parameters are listed in Table I.

Table 1: System Parameters

Governor time constant T_g	0.1
Diesel engine time constant T_d	5.0s
Inertia constant M	0.15puMWs/Hz
Damping constant D	0.008puMW/Hz
Speed droop R	3.0Hz/pu
Battery time constant T_b	0.1s
Blade radius R_w	14m
Inertia coefficient J	62.993 kgm^2
Air density ρ	1.225kg/m^3
Rated output P_{wg}	350kw
Phase voltage V	692.82v
Stator resistance R_1	0.00397Ω
Stator reactance X_1	0.0376 Ω
Rotor resistance R_2	0.0043 Ω
Rotor reactance X_2	0.0534 Ω

Control design

Our main approach is to define robustness where we include some uncertainties, disturbance signals and performance weights. Fig.5 shows the interconnected system where uncertainty of 5% is added to diesel block and 3% is added to rotating mass and load [12]. There are three control signals in our model. One is for diesel engine, the second one is for battery control and the third one is for maintaining the battery's SOC to 50%. We also include some disturbance signals at the summing junction as these occurs due to load and WTG output fluctuations. There arises a proper selection of performance weights as it relays on system robustness. Since the low frequency load deviations are handled by conventional generator and high frequency load deviations are taken up by battery, our controller should be designed accordingly. Also it should maintain battery SOC. So, the performance weights on error signals for generator, battery and SOC are taken as,

$$W_g^e = \frac{20}{s+0.0001} \tag{6}$$

$$W_b^e = \frac{20s+1}{s+0.0001} \tag{7}$$

$$W_{soc}^e = \frac{50s+0.001}{0.5s+0.1} \tag{8}$$

The control input weights are also designed for conventional generator and battery which are stated as

$$W_g^c = \frac{s+0.1}{5s+1} \tag{9}$$

$$W_b^c = \frac{0.2s+0.1}{100s+0.1} \tag{10}$$

By proper selection of these weights, our controller can handle uncertainities in the plant.

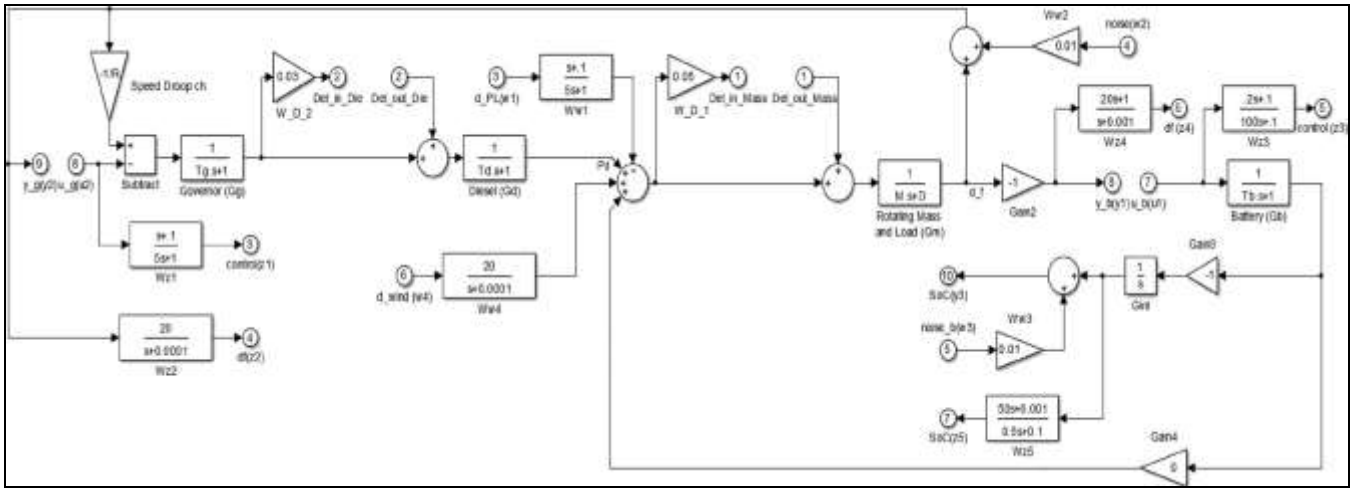

Fig 5: Plant model

***μ*-synthesis controller design**

We consider the feedback control system shown in Fig.6**,** with the generalized plant *P*, the controller *K*, and the uncertainty block Δ, where Δ = diag(Δ_i). Here, *w* is the exogenous input vector, *z* is the exogenous output vector, *y* is the measured output vector, and *u* is the control input vector to the generalized plant [10]. The system robustness can be estimated from the smallest structured value Δ which makes the matrix I-MΔ singular at any given frequency. Computing this value for all frequencies we can determine the smallest destabilizing perturbation, and hence the system robustness. This metric is termed as structured singular value (denoted as μ), which stated mathematically is defined for a matrix M stated as:

$$\mu(M) = \frac{1}{\min_{\Delta}\langle \sigma(\Delta) | \det(I - M\Delta) = 0 \rangle} \tag{11}$$

Where M is the lower linear fractional transformation (LFT) of P and K, and Δ = diag(Δ_i) is block diagonal.

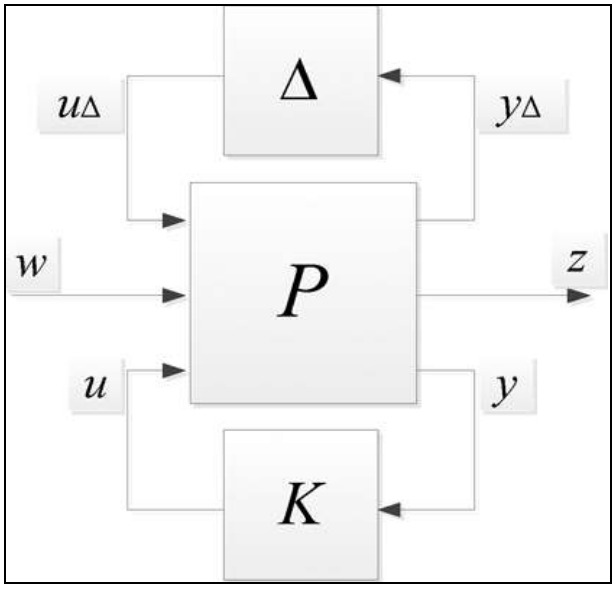

Fig 6: Control configuration for μ-synthesis

There are 12 first order transfer functions indicating 12 states in the system. It is to be noted that the system already contains dynamic uncertainties, weighting functions which set the robustness specification. The state-space

representation (matrices A, B, C, D) of the linearized plant is obtained by MATLAB command *'linmod'*. A D-K iteration algorithm is used for designing µ-synthesis controller. This iterative method is the combination of *h*-infinity and µ-analysis where both robustness to uncertainty and enhanced performance can be obtained.

Fractional-order PID controller

The concept of fractional order controller deals with differential equations using fractional calculus which is nothing but the generalisation of the ordinary calculus. The commonly used definition for fractional differential-integral is given by Riemann-Liouville (R-L) definition which is stated as [11],

$$ {}_aD_t^{\lambda} = D^n J^{n-\lambda} f(t) = \frac{1}{\Gamma(n-\lambda)} \left(\frac{d}{dt}\right)^n \int_a^t \frac{f(\tau)}{(t-\tau)^{\lambda-n+1}} d\tau \quad (12) $$

Where *a* and *t* are the limits of the operation, λ is the fractional order which can be complex number, *J* is the integral operator, *n* is the first integer which is not less than λ i.e., $n\text{-}1 \le \lambda \le n$ and Γ is the gamma function.

The common form of FOPID controller is $PI^{\lambda}D^{\mu}$ where λ and µ are order of integration and derivation which can be in any form and is shown in Fig 7. The transfer function of fractional order PID controller is

$$ c(s) = \frac{U(s)}{E(s)} = K_P + \frac{K_I}{S^{\lambda}} + K_D S^{\mu}, (\lambda, \mu \ge 0) \quad (13) $$

Where C(s) is the controller output, U(s) is the control signal, E(s) is the error signal. K_P, K_I and K_D are proportional, integral and derivative gain constants.

For µ=λ=1 PID controller is obtained, for µ=0 and λ=1 PI controller is obtained, for µ=1 and λ=0 PD controller is obtained. The main advantage of FOPID controller is less complexity in achieving control parameters and less sensitive to changes in parameters in the control system.

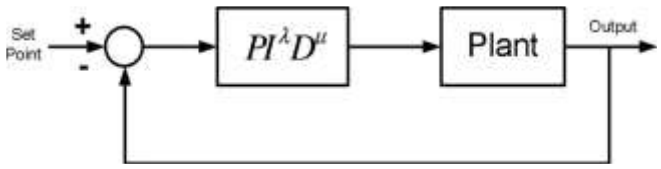

Fig 7: Block diagram of FOPID controller

Sliding Mode Control (SMC)

Sliding mode control (SMC) is a nonlinear control technique exhibiting tremendous possessions of accuracy, robustness, easy tuning and implementation [8]. SMC systems are designed to drive the system states onto a particular surface in the state space called as sliding surface. Once the sliding surface is reached, sliding mode control keeps the states on the vicinity of the sliding surface. Hence the SMC is a two part controller design. The first part implicate the design of a sliding surface so that the sliding motion satisfies design specifications. The second deals with the selection of a control law that makes the switching surface attractive to the system state. The main aim is to make output variable y to a desired value y_d i.e, the output error variable e = y - y_d is made to zero approximately after a transient of admissible time.

Consider the nonlinear SISO system,

$$ \dot{X} = f(x,t) + g(x,t)u \quad (14) $$

$$ y = h(x,t) \quad (15) $$

Where, u is the scalar input variable and y is the scalar output variable. Here $x \in R^n$ denotes the state vector. As mentioned earlier, SMC has two phases. The first phase i.e, 'sliding surface design' has a scalar function which is represented as $\sigma(x): R^n \to R$, as sliding surface depends on error e_y with certain number of its derivatives $\sigma = \sigma\left(e, \dot{e}, \cdots, e^k\right)$. The function σ is made zero making stable differential equation of any solution to zero accordingly. From geometrical point of view, the equation σ=0 defines a surface in the error space called as 'sliding surface'. The orbits of the controlled system are forced onto the sliding surface where the system behaviour meets the design specifications.

The second phase i.e, 'control input design' is to finding a control action that is able to make σ variable to zero in finite time.

Simulation results

The simulation results for the µ-synthesis, PID, FOPID and SMC controllers are discussed. In fig.8 load and wind turbine generator output variations are shown where power variations are represented in per unit with respect to time in seconds. Fig.9 shows the frequency variations using µ-synthesis controller with maximum battery power. It can be observed that frequency deviation (del f) is within 1% as for microgrids, changes in frequency should be within 1% else breaker contact gets tripped resulting discontinuity of the supply.

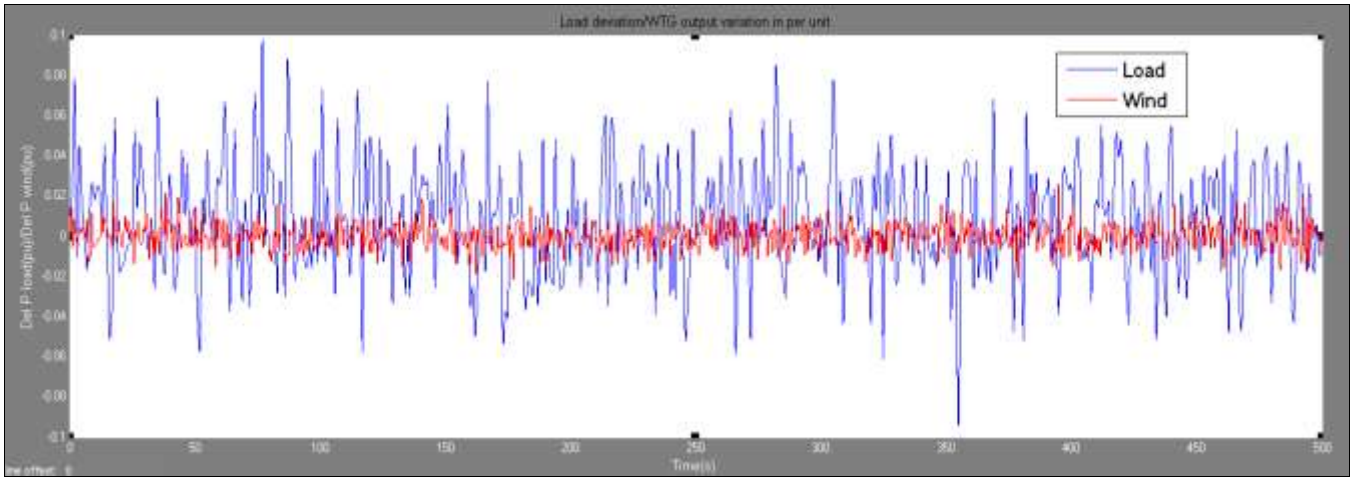

Fig 8: Power variations of load and wind

Fig 10 shows the power variations of load, generator, wind and battery whereas fig.12 shows the power variations without battery. On comparing results of these two figures, more frequency deviation is occurred when no battery is used whereas less than 1% of frequency variation is obtained when 3% and 100% battery power is used which is shown in fig.11.

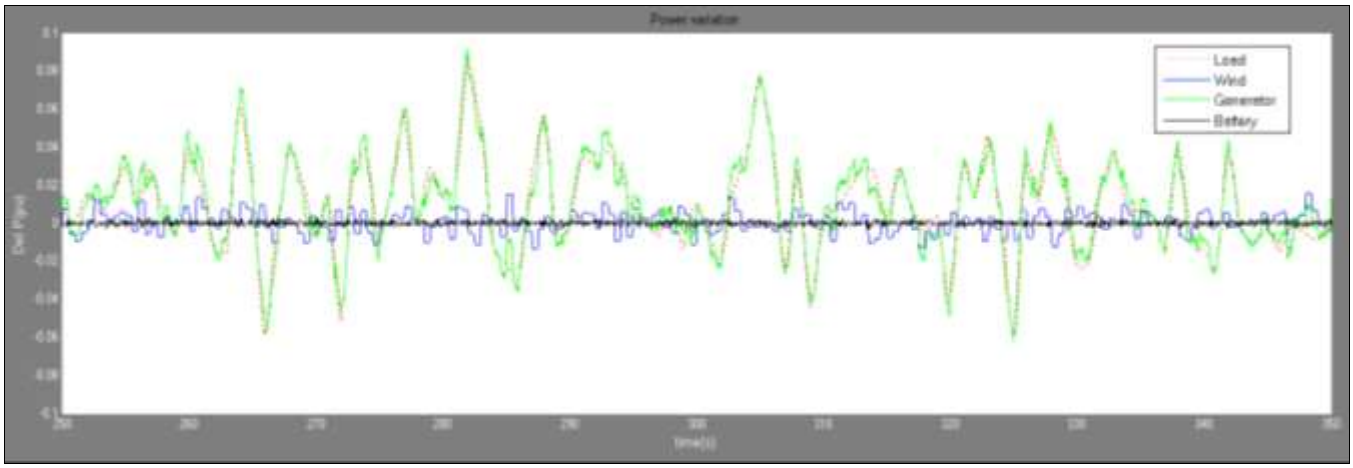

Fig 9: Power variation with maximum battery power

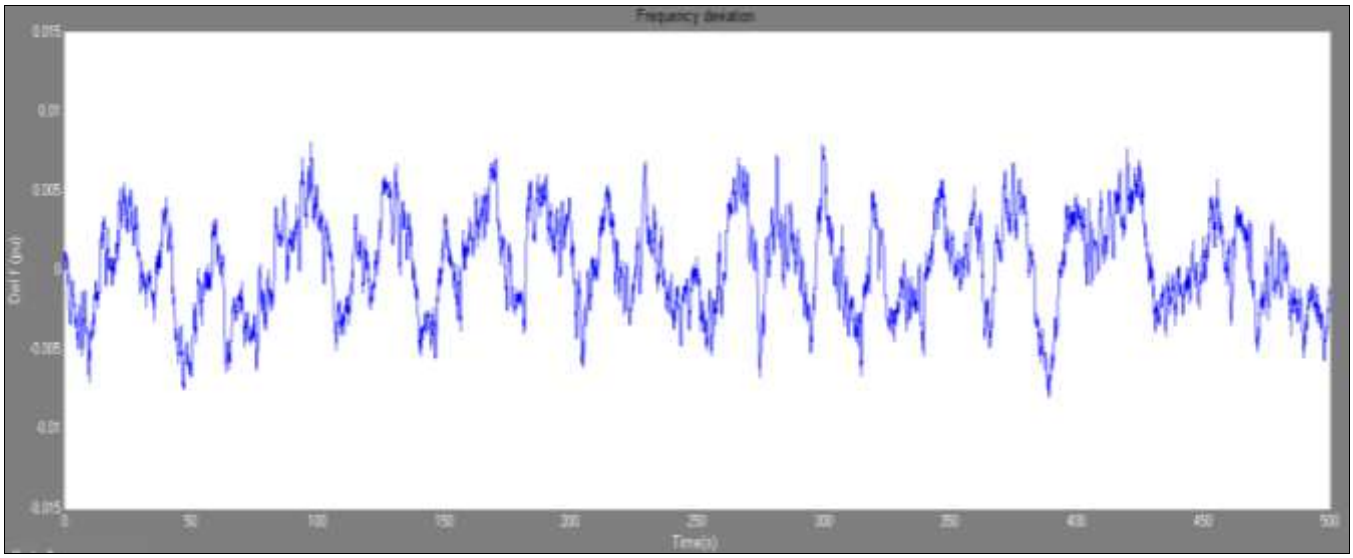

Fig 10: Frequency variations using µ-synthesis

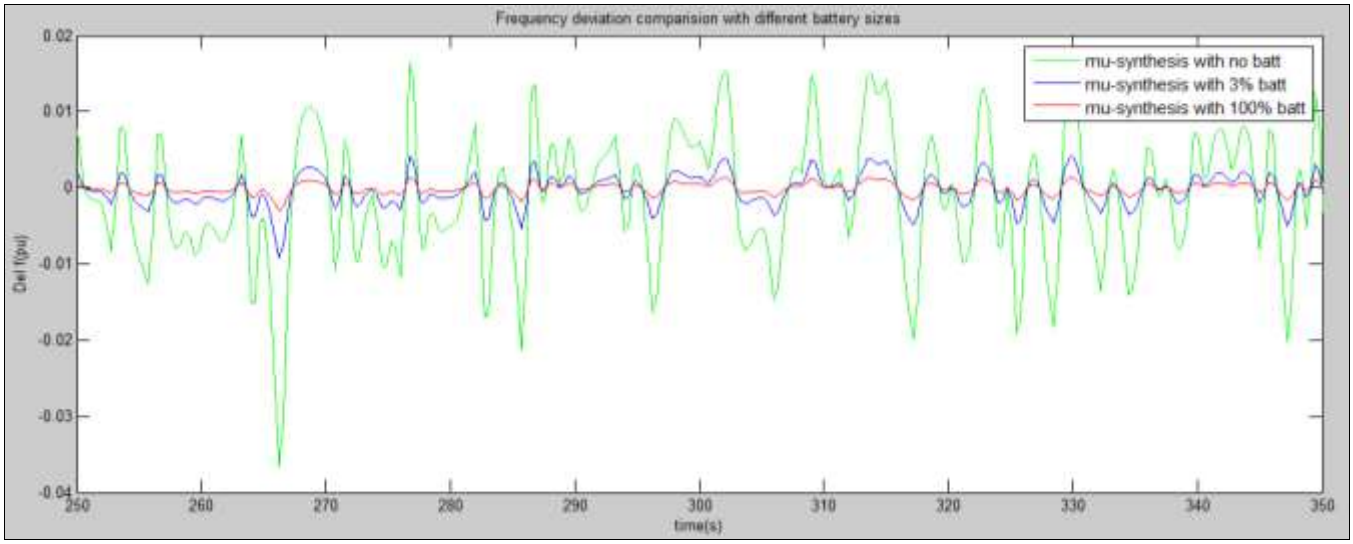

Fig. 11 Frequency variations with different battery sizes

Fig.13 shows the frequency variation comparison between µ-synthesis and PID when full battery power is used. PID controller is tuned without uncertainties and disturbance signals. A Ziegler-Nichols method is used for tuning PID. Better results are obtained when µ-synthesis controller is used as compared to PID controller. Our estimation is to determine the robustness of the system. Hence, we add 10% noise to the system. It can be seen that PID controller is not capable of controlling frequency variations whereas µ controller provide better performance which is shown in Fig.14.

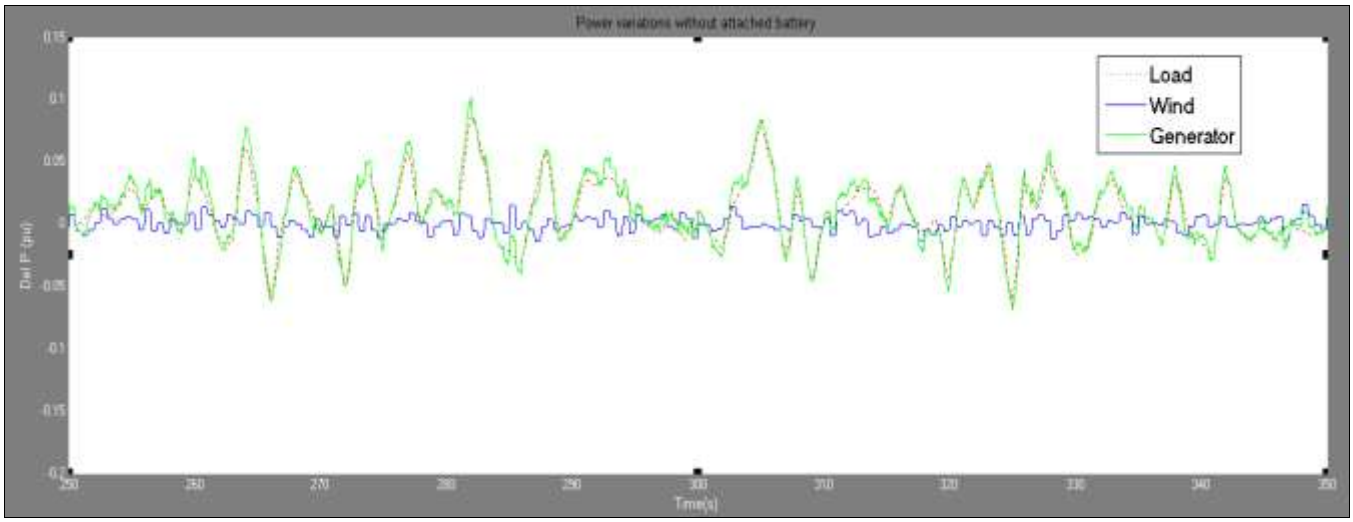

Fig 12: Power variations without battery storage system

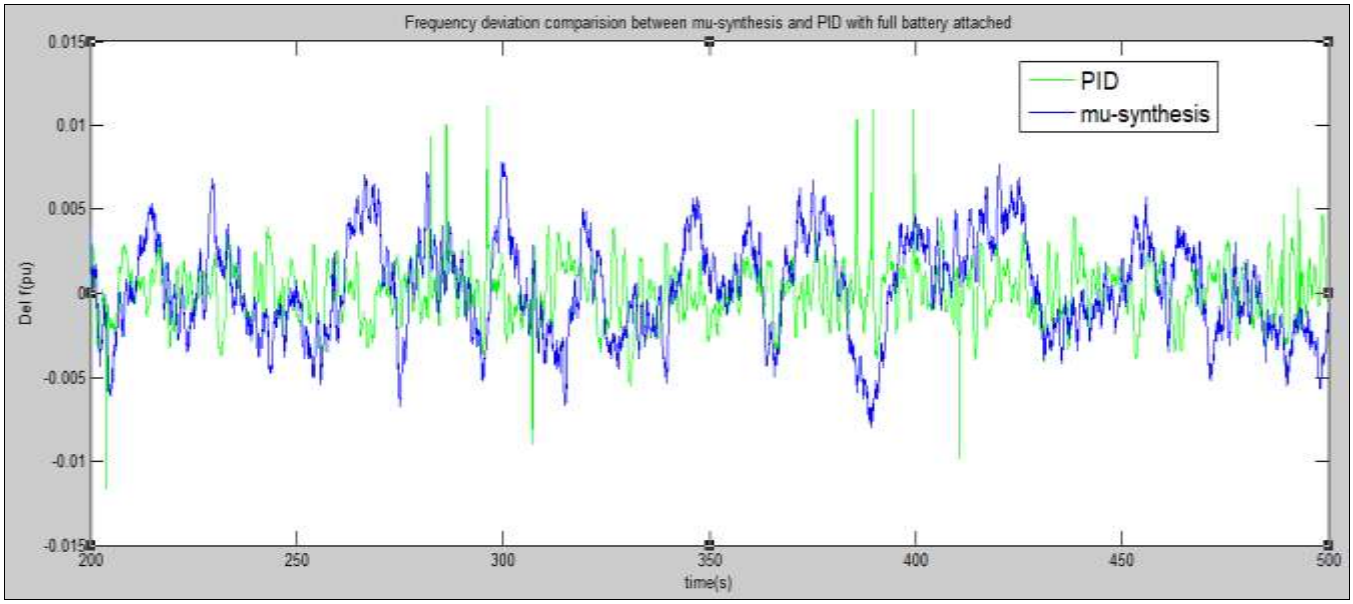

Fig 13: Frequency variation comparision between µ-synthesis and PID

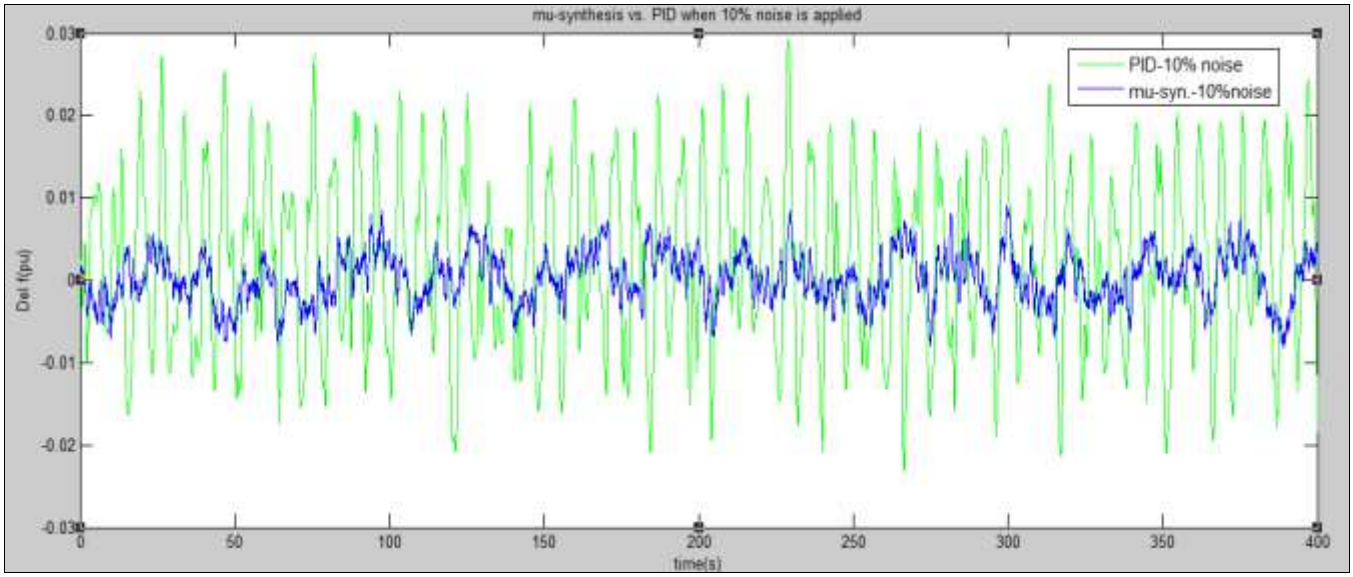

Fig 14: Frequency deviation comparison between µ-synthesis and PID with 10% noise

The main drawback of µ-synthesis controller is proper selection of performance weights. If we choose the control signal performance weight as equation (16) instead of equation

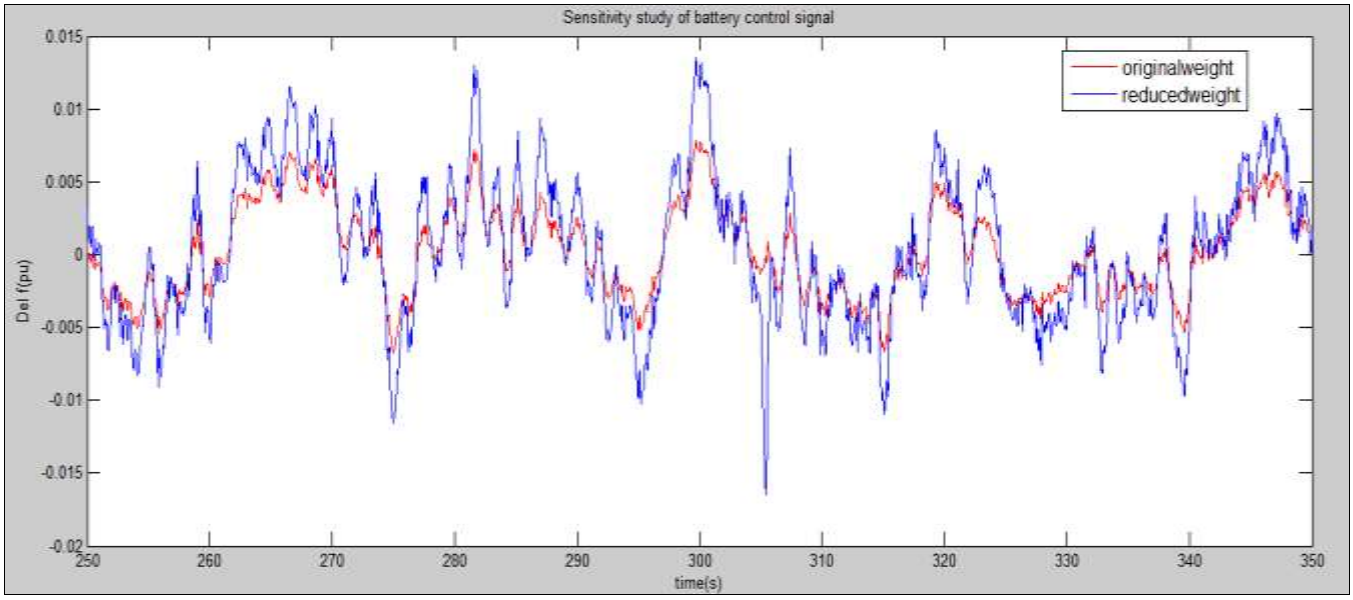

Fig 15: Frequency deviations comparison with different weights on battery control signal

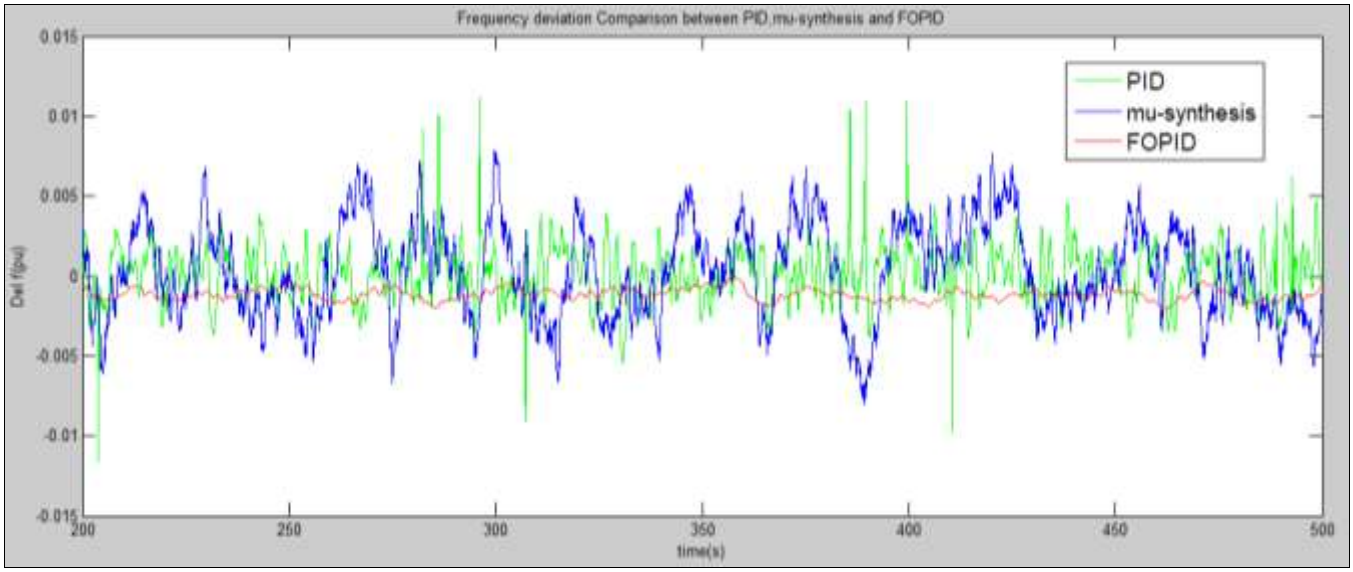

Fig 16: Frequency deviation comparison between PID, µ-synthesis and FOPID

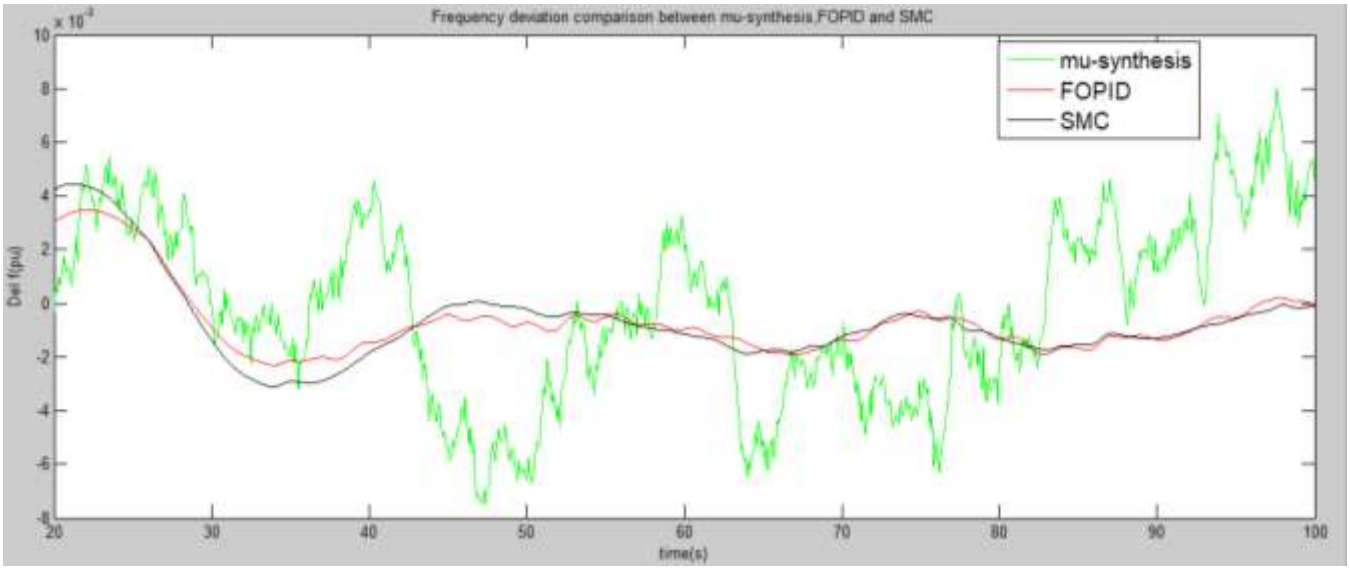

Fig 17: Frequency deviation comparison between µ-synthesis, FOPID and SMC

(17) a major frequency variations is obtained which is shown in Fig.15.

$$W_b^c = \frac{2s+0.1}{1000s+0.1} \quad (16)$$

$$W_b^c = \frac{0.2s+0.1}{100s+0.1} \quad (17)$$

Fig. 16 shows the performance of µ-synthesis, PID and FOPID where better results are obtained by using FOPID controller. Also fig.17 shows the comparison of µ-synthesis, FOPID and SMC controller where frequency variations are reduced further. Performance indices for various controllers are calculated in the table 2, where IAE is integral of absolute error, ISE is integral of squared error, ITAE is integral of time multiply absolute error, ITSE is integral of time multiply squared error.

Table 2: Performance indices

	IAE	ISE	ITAE	ITSE
PID Controller	2.3302e+007	7.7704e+009	1.4505e+012	5.4396e+014
µ-synthesis controller	2.3302e+007	7.7704e+009	1.4499e+012	5.437e+014
FOPID Controller	3.8180e+010	1.2728e+012	3.8893e+012	1.4585e+015
SMC	8.0014e+006	2.1336e+008	2.1339e+012	6.4017e+013

Conclusion

In this paper, we designed µ-synthesis, PID, FOPID and SMC controller for reducing frequency deviations in a microgrid containing conventional generator, load, wind turbine generator and battery energy storage system. It is observed that SMC controller provide better performance as compared to all other controllers irrespective of system disturbances. Low frequency load variations are handled by conventional generator and high frequency load variations are handled by battery energy storage system by charging and discharging. It should be noted that battery SOC must be kept around 50% and our controller could be able to do it.

References

1. Lu J, Niu M. Overview on microgrid research and development. In: Zhu R, *et al*., editors. ICICA, part I, CCIS 105. Berlin Heidelberg: Springer-Verlag; 2010. p. 161-8.
2. Howlader AM, Izumi Y, Uehara A, Urasaki N, Senjyu T, Yona A, *et al*. A minimal order observer based frequency control strategy for an integrated wind-battery-diesel power system. Energy. 2012;46(1):168-78.
3. Goya T, Omine E, Kinjyo Y, Senjyu T, Yona A, Urasaki N, *et al*. Frequency control in isolated island by using parallel operated battery systems applying h-inf; control theory based on droop characteristics. IET Renew Power Gener. 2011;5:160-6.
4. Sundaram V, Jayabarathi T. Load frequency control using PID Tuned ANN controller in power system. In: Proc. 1st Int Conf Electrical Energy Syst (ICEES); 2011. p. 269-74.
5. Dhanalakshmi R, Palaniswami S. Application of multi stage fuzzy logic control for load frequency control of an isolated wind diesel hybrid power system. In: Proc. Int Conf Green Technol Environmental Conservat (GTEC); 2011. p. 309-15.
6. Wang ZQ, Sznaier M. Robust control design for load frequency control using /spl mu/-synthesis. In: Proc. Southcon/94 Conf Rec.; 1994. p. 186-90.
7. Alomoush MI. Load frequency control and automatic generation control using fractional-order controllers. Electr Eng. 2010; pp. 357–68. DOI:10.1007/s00202-009-0145-7.
8. Bevrani H. Robust power system frequency control. New York, NY: Springer Science+Business Media, LLC; 2009.
9. Bevrani H. Robust load frequency controller in a deregulated environment: synthesis approach. In: Proc. IEEE Int Conf Control Appl. 1999;1:616-21.
10. Shah P, Agashe S. Review of fractional PID controller. Mechatronics. 2016;38:29-4.
11. Han Y, Young PM. Robust control for microgrid frequency deviation reduction with attached storage system. IEEE Trans Smart Grid. 2015;6(2).
12. Shariatzadeh F, Kumar N, Srivastava A. Optimal control algorithms for reconfiguration of shipboard microgrid distribution system using intelligent techniques. IEEE Trans Ind Appl. 2017;53(1):474-82.
13. Khooban MH, Niknam T, Blaabjerg F, Dragičević T. A new load frequency control strategy for micro-grids with considering electrical vehicles. Elect Power Syst Res. 2017;143:585-98.
14. Pahasa J, Ngamroo I. Coordinated control of wind turbine blade pitch angle and PHEVs using MPCs for load frequency control of microgrid. IEEE Syst J. 2016;10(1):97-105.
15. Jin Z, Sulligoi G, Cuzner R, Meng L, Vasquez JC, Guerrero JM *et al*. Next-generation shipboard DC power system: introduction smart grid and DC microgrid technologies into maritime electrical networks. IEEE Electrific Mag. 2016;4(2):45-57.
16. Chandragupta Mauryan KS, Naresh M, Parthasaradhy P. Intelligent system design for demand side management in smart grid. Sci Bull. 2022;84(2):173-84.
17. Chandra Gupta Mauryan KS, Purrnimaa Shiva Sakthi R. Design and development of hybrid power generation model for micro-grid applications. J Adv Res Dyn Control Syst. 2019;11(6):379-85.
18. Chandra Gupta Mauryan KS, Purrnimaa Shiva Sakthi R. Smart grid implementation in improving power stability for home energy management and demand response using renewable energy sources. J Huazhong Univ Sci Technol. 2021;50(6):01-14.
19. Chandragupta Mauryan KS, Abuvatamizhan M, Balaji V, Mani R. Improved efficiency of large capacity renewable energy - integration with grid. Int J Eng Sci. 2014;3:12-7.
20. Chandragupta Mauryan KS, Nivethitha T, Yazhini B, Preethi B. Study on integration of wind and solar energy to power grid. Int J Eng Res Appl. 2014;4:67-71.